Supporting Information for "The Role of Mechanical Force on the Kinetics and Dynamics of Electrochemical Redox Reactions on Graphene".

Shivaranjan Raghuraman[a], Mohammadreza Soleymaniha[a], Zhijiang Ye[b] and Jonathan R. Felts[a]*.

[a]Advanced Nanomanufacturing Laboratory, Department of Mechanical Engineering, Texas A&M University, College Station, Texas – 77843-3123.

[b]Ye Research Group, Department of Mechanical and Manufacturing Engineering, Miami University, Oxford, Ohio – 45056.

KEYWORDS Atomic Force Microscopy, Electrode Kinetics.

TWO STEP ROUTINE TO OBTAIN RELATIVE FRICTION

We implemented a two step routine to obtain friction of electrochemically modified areas with respect to that of pristine surrounding graphene (see supplemental movies). First, a 250x250 nm "drive scan" with voltage bias and applied tip force dictated by the experimental conditions deposits oxygen. A subsequent 625x625 nm "measure scan" monitors the friction change. The friction values of the electrochemically modified region (blue square in figure) with respect to the friction of surrounding graphene area (red square in figure) gives relative friction. This constitutes one single data point of an overall reaction curve (figure 2 main). The spring constant of the tip was calibrated using the thermal tuning method and was 1.37±0.24 N/m based on several calibrations, where the error reported here is the combination of uncertainty from calibration procedure and variability between tips.[1]

CURRENT ESTIMATION

For the one electron transfer process considered in the study, the total current involved in depositing oxygen over the surface can be calculated as,

$$I_{tot} = e \times \frac{dn}{dt} \qquad (1)$$

Where, n is the total number of active sites in the given scan area. As a graphene unit cell has 2 carbon atoms accounting for sharing and an area of $0.05\,nm^2$, a scan size of $250\,nm^2$ contains 2,500,500 carbon atoms. However, several studies show that even at a theoretical maximum functionalization of graphene, a significant fraction of the carbon atoms would have functional groups attached. Nevertheless, for a conservative estimate, n was assumed to be equal to the number of carbon atoms. The time per scan t is 15s and charge of an electron e is $1.6 \times 10^{-19}\,C$.

As friction directly correlates to composition, the maximum friction observed can be attributed to a fully oxygenated surface. Accordingly, the current per scan can be calculated as,

$$I_{Scan} = \frac{\Delta f}{f_{max}} \times I_{tot} \qquad (2)$$

Where, Δf is the change in friction per scan and f_{max} is the maximum value of friction observed during the reaction. For the reaction curve in fig 2A, the current was observed to be on the order of one fA. It can be seen that the derivative shown in fig 2B correlates well to the estimated current (fig 2C) and a peak of the derivative corresponds to the maximum current during the reaction.

EXPRESSION FOR ACTIVATION BARRIER

The potential energy profile for an electrochemical reaction modified by force can be given as,

$$V_r(x) = \frac{x^2}{\gamma_r} - Fx - n_e F_c V \qquad \textit{(3 – same as 3 main)}$$

$$V_p(x) = \frac{\left(x - \Delta x_o^{\ddagger}\right)^2}{\gamma_p} + \Delta G_o - Fx \qquad \textit{(4 – same as 4 main)}$$

where, $V_r(x)$ is the reactant energy profile, $V_p(x)$ is the product energy profile, F is the applied force, x is the reaction coordinate, γ_r and γ_p are the curvatures of the reactant and product profiles respectively, n_e is the number of electrons transferred, F_c is Faraday's constant, $\Delta x_o^{\ddagger}$ is the reaction path length, ΔG_0 is the standard Gibb's Free energy for the reaction and V is the applied voltage.

The activation barrier for this reaction (E_{eff}) is the energy difference between the transition state i.e. $V_r(x_{max})$ and the reactant minimum i.e. $V_r(x_{r,min})$.

$$E_{eff} = V_r(x_{max}) - V_r(x_{r,min}) \qquad \textit{(5 – same as 5 main)}$$

Here by setting $\frac{\partial V_r}{\partial x} = 0$, $x_{r,min}$ can be given as,

$$x_{r,min} = \frac{F\gamma_r}{2} \qquad \textit{(6 – same as 6a main)}$$

By equating the reactant and product energy potentials (eqn 3 in main and 4 in main), x_{max} can be given as,

$$x_{max} = \frac{\gamma_r \phi}{\gamma_p - \gamma_r} \qquad (7)$$

where,

$$\phi = \Delta x_o^{\ddagger} + \gamma_p \sqrt{\frac{\left((\Delta x_o^{\ddagger 2} + (\Delta G_0 - n_e F_c V)(\gamma_p - \gamma_r)\right)}{\gamma_r \gamma_p}} \qquad (8)$$

Therefore, the energy at the reactant minimum and transition state can be expressed as,

$$V_r(x_{r,min}) = -\frac{\gamma_r F^2}{4} - n_e F_c V \qquad (9)$$

$$V_r(x_{max}) = \frac{\gamma_r \phi^2}{(\gamma_p - \gamma_r)^2} - n_e F_c V + \frac{F\gamma_r \phi}{\gamma_p - \gamma_r} \qquad (10)$$

By substituting eqn 9 and 10 into eqn 5, the effective energy barrier can be obtained as,

$$E_{eff} = \frac{\gamma_r \phi^2}{(\gamma_p - \gamma_r)^2} + \frac{F\gamma_r \phi}{\gamma_p - \gamma_r} + \frac{\gamma_r F^2}{4} \qquad (11)$$

The expression for effective energy barrier is quite cumbersome and assuming equal curvatures for the reactant and product profiles, i.e. $\gamma_r = \gamma_p$ will simplify the expression greatly. The modified expression for the energy barrier is therefore,

$$E_{eff} = E_a + \alpha(F_N, V) n_e F_c V - \psi(F_N) \qquad (12 – same as 7 main)$$

$$E_a = \left[\frac{\Delta x_o^2}{4\gamma} + \frac{\Delta G_o}{2\gamma^2} + \frac{\Delta G_o^2}{4\Delta x_o^2 \gamma^2}\right] \qquad (12a – same as 7a main)$$

$$\alpha(F_N, V) = \left[\frac{1}{2} + \frac{\gamma \Delta G_o}{2\Delta x_o^2} - \frac{\gamma F}{2\Delta x_o} + \frac{\gamma n_e F_c V}{4\Delta x_o^2}\right] \qquad (12b – same as 7b main)$$

$$\psi(F_N) = \left[\frac{\Delta x_o}{2} + \frac{\gamma \Delta G_o}{2\Delta x_o}\right] F + \left[\frac{\gamma}{4}\right] F^2 \qquad (12c – same as 7c main)$$

PROCEDURE TO OBTAIN KINETICS AND DYNAMICS PARAMETERS:

1) The reaction curve obtained through voltage ramps at a given applied tip load can be described by (see main paper "Experimental Methods"),

$$\int_0^f \frac{df}{f^n} = \frac{A}{\zeta} \int_0^V e^{\frac{E_{eff}(F_N, V)}{RT}} dV \qquad (13 – same as 12main)$$

2) For a first order reaction, integrating equation 19 yields,

$$\ln(-\ln(1 - f)) = Q_1 + Q_2 V \qquad (14 – same as 13 main)$$

Plotting $\ln(-\ln(1-f))$ against V results in a straight line with slope Q_2 and intercept Q_1 (see figure 4b in main).

$$Q_1 = ln(-\left(\frac{ART}{\zeta\alpha(F_N,V)n_eF_c}\right) - \frac{E_a - \psi(F_N)}{RT} \quad \textit{(15 – same as 14 main)}$$

$$Q_2 = -\left(\frac{\alpha(F_N,V)n_eF_c}{RT}\right) \quad \textit{(16 – same as 15 main)}$$

3) The value of $\alpha(F_N,V)$ can be obtained from the slope Q_2 by substituting known values ($n_e = 1, F_c = 96485.232\frac{C}{mol}, R = 8.314\frac{J}{mol.K}$ $and\ T = 300K$ $(room\ temperatue)$. The value of $E_a - \psi(F_N)$ can be obtained from intercept Q_1 by substituting $\alpha(F_N,V)$ assuming a value for attempt frequency (A=1e13/s).[2, 3] A voltage ramp rate of ζ = -58.33 V/s was used throughout our work (see SI section on effective voltage ramp rate).
4) Combining the explicit forms of E_a and $\psi(F_N)$ from equation 12a and 12c we obtain,

$$E_a - \psi(F_N) = \left[\frac{\Delta x_o^2}{4\gamma} + \frac{\Delta G_o}{2\gamma^2} + \frac{\Delta G_o^2}{4\Delta x_o^2\gamma^2}\right] - \left[\frac{\Delta x_o}{2} + \frac{\gamma\Delta G_o}{2\Delta x_o}\right]F - \left[\frac{\gamma}{4}\right]F^2 \quad \textit{(17)}$$

5) By fitting eq.17 with a second order polynomial, the stiffness of the potential (γ) can be calculated from the quadratic term.
6) By fitting eq. 12b with a straight line, the value of the path length (Δx_o) can be calculated from the slope.
7) In local anodic oxidation experiments such as ours, the potential drop for each half reaction cannot be directly determined experimentally. In theory, the voltage offset originates from the standard electrode potential of platinum tip (1.18V) and the resistance from the water meniscus. The resistance of water meniscus depends on the local composition and density of water in contact thus making it difficult to estimate accurately. However, we can fit for the overpotential from the value of standard Gibbs Free Energy Change (ΔG_0) which can be calculated from the first order term of the quadratic fit to eq 17. The standard Gibbs free energy (ΔG_0) for water splitting has been theoretically and experimentally shown to be around 1.2 eV. We use this fact to fit for overpotential and estimate a voltage offset of -2.2V that yields a corresponding ΔG_0 of 1.2 eV. This offset was then propagated into the experimentally applied voltage bias values to obtain the corrected values of the effective symmetry factor ($\alpha(F_N,V)$) and effective energy barrier ($E_{eff}(F_N,V)$) shown in figures 6a and 6b.

CAPACITIVE FORCES

A conductive AFM tip experiences electrostatic force under an applied electric field in addition to the applied tip load. The capacitive force varies with applied voltage and can be mathematically expressed as[4],

$$F_{cap} = -\pi\epsilon_0 V^2 \left(\frac{R}{z + \frac{h}{\epsilon}} \right) \quad (18)$$

Here, h is the height of the water meniscus and has been observed to be around 400 nm at 60% relative humidity[5], ϵ_0 is the permittivity of free space and is $8.8541 \times 10^{-12} m^{-3} kg^{-1} s^4 A^2$, V is the applied voltage and ranges between -2 and -9 V for our experiments, R is the tip radius, z is the distance between tip and meniscus and ϵ is the relative dielectric constant of water and is 80. For a tip radius of 50 nm, and for -2 to -9 V applied voltage range, the capacitive force varies between 1.1 and 26.4 nN.

FINITE ELEMENT SIMULATIONS:

The tip-multilayer graphene-silicon interface was modelled to be axisymmetric about the y-axis as shown in figure 3A. The interaction between the tip and graphene atoms were described using standard Lennard Jones potentials, where the applied tip force was controlled by tuning the interatomic separation.[6-8] Studies have shown that applying a force using an AFM tip causes the top layer graphene to pucker or deform out of plane around the tip as seen in figure 3A. This induces strain in the graphene lattice which is high around the contact and decreases with distance away from the contact line. Figure 3B shows the total strain on the top layer of graphene as a function of distance away from the tip for 17, 23 and 47 nN applied load. In each case, the maximum strain occurred at the center of the tip and decreased away from the tip. In addition to the force applied on atoms, the induced strain can alter the local reactivity of the carbon atoms. While this effect is not actively decoupled in our experiments, the influence of strain on chemical reactivity and barrier to oxygen adsorption can be neglected in comparison to the effect of applied stress in our study.

FIGURES

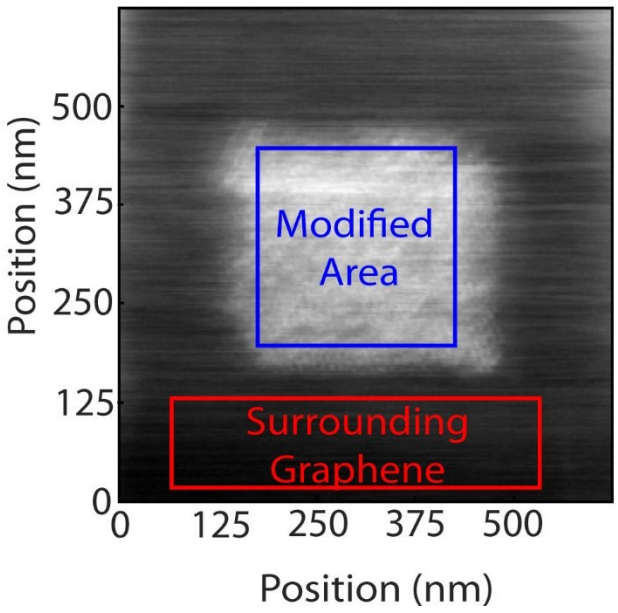

Figure 1 A sample Friction Image obtained during LAO. Friction of the modified area with respect to that of surrounding graphene region gives Relative Friction. Bright areas indicate higher friction.

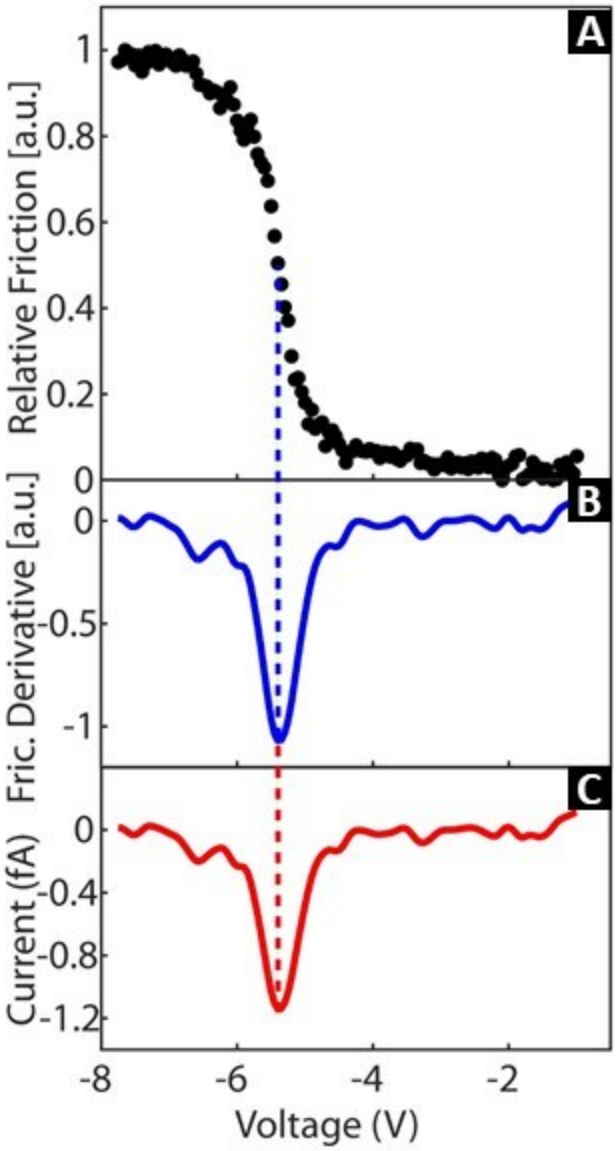

Figure 2: A. Reaction Curve, B. Derivative, C. Estimated current per scan.

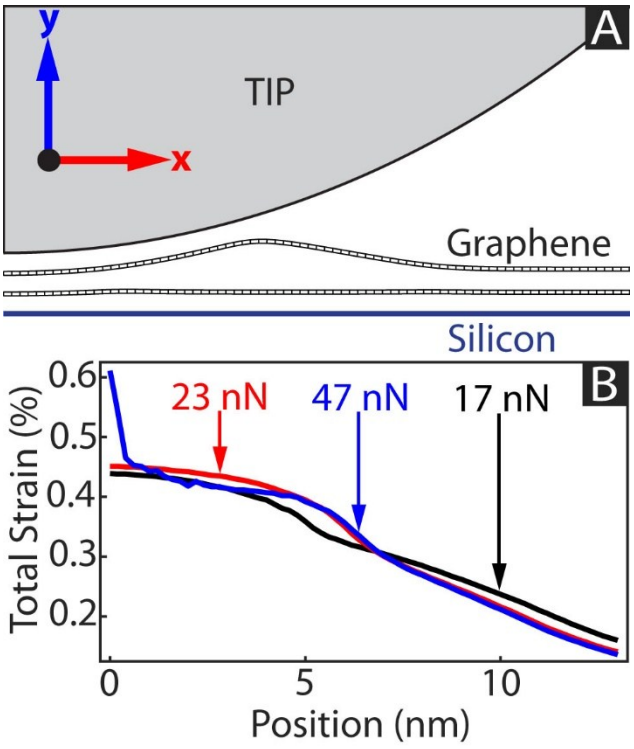

Figure 3: A. The simulation space shows tip, double layer graphene and silicon. In this particular simulation condition the tip applies a 23 nN force on the graphene. This causes the top layer to pucker up. B) Strain as a function of position along graphene for 17, 23 and 47 nN applied load conditions.

REFERENCES

1. Butt, H.-J.; Jaschke, M. *Nanotechnology* **1995,** 6, (1), 1.
2. Jacobs, T. D.; Carpick, R. W. *Nature nanotechnology* **2013,** 8, (2), 108.
3. Zhurkov, A. *Int. J. Fract. Mech.* **1965,** 1, 311-323.
4. Casuso, I.; Fumagalli, L.; Gomila, G.; Padrós, E. *Applied Physics Letters* **2007,** 91, (6), 063111.
5. Weeks, B. L.; Vaughn, M. W.; DeYoreo, J. J. *Langmuir* **2005,** 21, (18), 8096-8098.
6. Deng, Z.; Smolyanitsky, A.; Li, Q.; Feng, X.-Q.; Cannara, R. J. *Nature materials* **2012,** 11, (12), 1032.
7. Gong, P.; Li, Q.; Liu, X.-Z.; Carpick, R. W.; Egberts, P. *Tribology Letters* **2017,** 65, (2), 61.
8. Li, S.; Li, Q.; Carpick, R. W.; Gumbsch, P.; Liu, X. Z.; Ding, X.; Sun, J.; Li, J. *Nature* **2016,** 539, (7630), 541.